

Tropane and related alkaloid skeletons via a radical [3+3]-annulation process

Eloïse Colson¹, Julie Andrez², Ali Dabbous², Fabrice Dénès¹, Vincent Maurel²✉, Jean-Marie Mousesca²✉ & Philippe Renaud¹✉

Tropanes and related bicyclic alkaloids are highly attractive compounds possessing a broad biological activity. Here we report a mild and simple protocol for the synthesis of *N*-arylated 8-azabicyclo[3.2.1]octane and 9-azabicyclo[3.3.1]nonane derivatives. It provides these valuable bicyclic alkaloid skeletons in good yields and high levels of diastereoselectivity from simple and readily available starting materials using visible-light photoredox catalysis. These bicyclic aniline derivatives are hardly accessible via the classical Robinson tropane synthesis and represent a particularly attractive scaffold for medicinal chemistry. This unprecedented annulation process takes advantage of the unique reactivity of ethyl 2-(acetoxymethyl) acrylate as a 1,3-bis radical acceptor and of cyclic *N,N*-dialkylanilines as radical 1,3-bis radical donors. The success of this process relies on efficient electron transfer processes and highly selective deprotonation of aminium radical cations leading to the key α -amino radical intermediates.

¹Department of Chemistry, Biochemistry and Pharmaceutical Sciences (DCBP), University of Bern, Freiestrasse 3, CH-3012 Bern, Switzerland. ²Univ. Grenoble Alpes, CEA, CNRS, IRIG, SyMMES, F-38000 Grenoble, France. ✉email: vincent.maurel@cea.fr; jean-marie.mousesca@cea.fr; philippe.renaud@unibe.ch

Nitrogen-containing moieties are omnipresent in natural products, biologically active compounds and agricultural chemicals. In particular, the 8-azabicyclo[3.2.1]octane and 9-azabicyclo[3.3.1]nonane skeletons constitute the core of many natural tropane¹ and homotropane alkaloids², respectively, and analogues presenting a wide range of biological activities. For instance, tropinone, cocaine and scopolamine (Fig. 1) are amongst the most popular representative examples of natural alkaloids presenting a 8-azabicyclo[3.2.1]octane (tropane) skeleton as their base structure. Unlike its natural enantiomer, unnatural (–)-ferruginine (Fig. 1), is a good agonist for nicotinic acetylcholine receptor. The 9-azabicyclo[3.3.1]nonane (homotropane) skeleton can be found in the structure of (–)-adaline, and (+)-euphococcinine (Fig. 1)², two important defensive alkaloids from, respectively, the European ladybug *Adalia bipunctata* and the Australian ladybug *Cryptolaemis montrouzieri*. Moreover, *N*-arylated tropanes and related bicyclic aniline derivatives³ represent a particularly attractive scaffold for medicinal chemistry as illustrated by ACP 105^{4,5}, an orally available and potent selective androgen receptor modulator, and CFI-401870⁶, a single-digit nanomolar tyrosine threonine kinase (TTK) inhibitor (Fig. 1).

Since the report by Robinson of the multicomponent synthesis of tropinone based on a cascade Mannich reaction^{7,8}, access to tropanes and related alkaloids has been the object of intense activity⁹. Strategies based on ionic reactions, cycloadditions and transition metal mediated processes have been reported. The preparation of *N*-arylated tropane derivatives via Robinson synthesis is a knotty process¹⁰ with limited scope^{11–13} and they are mostly prepared via *N*-demethylation followed by a dubious *N*-arylation step¹⁴. Despite their attractiveness to build cycles, radical processes have only been scarcely used in tropane synthesis¹⁵. The development of a general and flexible access to tropane related heterocycles using a mild radical-based approach is expected to complement nicely the existing methods by allowing a direct preparation of *N*-arylated derivatives and by modifying the substitution pattern at position 3 of the tropane skeleton. To gain in efficiency, a cascade processes involving consecutive formation of C–C bonds is particularly sought. The biosynthesis of tropane alkaloids¹⁶ as well as Robinson biomimetic synthesis^{7,8} are both based on an ionic [3 + 3]-annulation processes involving 1,3-bis-iminium ions and 1,3-bis-enolates synthons (Fig. 2a). Inspired by this observation, we hypothesized that a radical version might be possible by using 1,3-bis- α -amino radical donor and 1,3-bis radical acceptor (Fig. 2b), radical donor

and acceptor being defined and represented according to Curran's proposal in his seminal article on retrosynthetic planning of radical reactions¹⁷. To the best of our knowledge, this type of radical [3 + 3]-annulation has not yet been reported^{18–24}.

The α -functionalization of tertiary amines has attracted much interest in the past and methods involving one- and two-electron oxidation pathway have been reported (Fig. 3). One-electron oxidation of the amine affords a nitrogen-centered radical cation. The oxidation leads to a massive increase of the acidity of the α -C–H bond relative to the starting amine²⁵. Rapid deprotonation of the radical cation gives the α -aminoalkyl radical that can be used for a variety of radical processes, such as for instance addition to alkenes leading to C–C bond formation (one-electron pathway)²⁶. On the other hand, the α -aminoalkyl radical is more easily oxidized than the starting amine and therefore further oxidation to the corresponding iminium ion can take place (two-electron pathway)²⁷. The iminium intermediate can be used for a variety of useful ionic transformations^{28,29}. As a consequence, the use of stoichiometric oxidants to perform radical reaction via the one-electron pathway is very challenging due to rapid overoxidation of the intermediate α -aminoalkyl radical to the corresponding iminium ion³⁰.

In this context, the single electron oxidation of amines *via* photoinduced electron transfer has been shown to be a suitable method to suppress this overoxidation. Mariano and co-workers reported in 1992 the photosensitized generation of α -aminoalkyl radicals from easily oxidized α -silyl amines and their subsequent

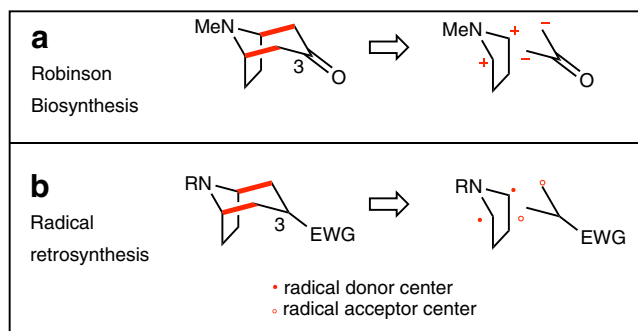


Fig. 2 Retrosynthetic analysis. Retrosynthetic analysis of tropane alkaloids according to their biosynthesis and to Robinson synthesis (a) as a source of inspiration for a radical retrosynthetic analysis (b). New C–C bonds are indicated in red, radical donor as red dot and radical acceptor as red circle.

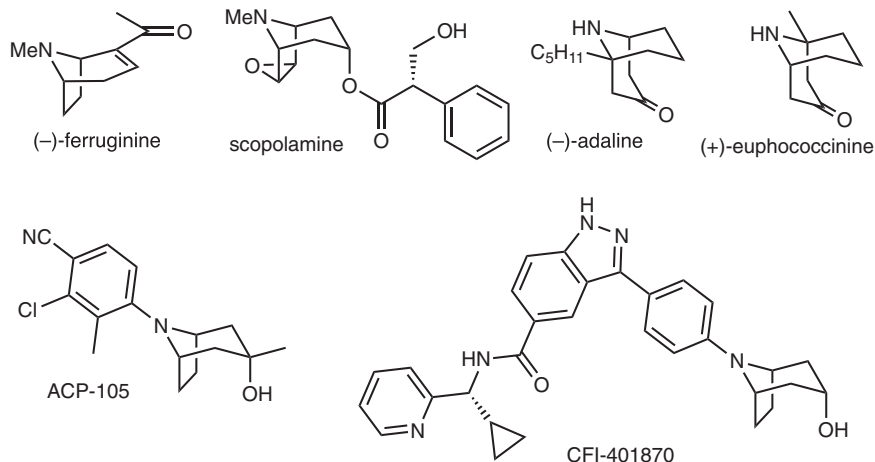


Fig. 1 Tropanes and homotropanes. Selected examples of tropane and homotropane alkaloids as well as *N*-arylated tropane derivatives of biological interest.

intra- and intermolecular additions to electron-poor olefins. Interestingly, they reported a 6-*endo*-trig cyclization process (Fig. 4a)³¹. Pandey took also advantage of the oxidation of a bis- α -silylamine to generate an azomethine ylide that can be used in 1,3-dipolar cycloaddition³². Pandey, Reiser et al.³³ and Nishibayashi^{26,34} independently extended this chemistry to photoredox-mediated protocols not only on α -silylated amines but also respectively on *N*-aryl-tetrahydroisoquinolines³³ and on cyclic and acyclic amines. Nishibayashi et al. reported the formation of bis-alkylated product starting from symmetrical starting materials, demonstrating that the intermediate mono-alkylated product has a similar reactivity as the starting amine under specific reaction conditions (Fig. 4b)³⁴. In 2014, MacMillan et al. reported the α -vinylation of aniline derivatives and *N*-Boc-protected amino acids using vinyl sulfones as coupling partners (Fig. 4c)³⁵. In this case, no bis-vinylation was reported

presumably due to the excess of the starting amine used under their conditions. The same year, Li and co-workers reported the first α -allylation of *N*-aryl tertiary amines using an allylic radical trap³⁶. Double addition to the radical trap was observed in one case albeit in very moderate yield (Fig. 4d). In 2020, Ready et al. reported a method for the regioselective α -functionalization of tertiary amines. Interestingly, the initially formed α -alkylation product could be further alkylated in a one-pot sequence (Fig. 4e)³⁷. The second alkylation takes place in a regioselective manner at the aliphatic position over the benzylic position. In one example, they observed the formation of a remarkable [3 + 3] adduct (Fig. 4e). In this reaction, the initial radical adduct is presumably abstracting a hydrogen from the benzylic position. Reduction of the benzylic radical followed by nucleophilic displacement of the Evans auxiliary account for product formation. All these results incited us to examine annulation reactions based on the double activation of tertiary amines. We described here a tandem process for the synthesis of tropane and homotropane alkaloid skeletons (Fig. 4f). The reaction is based on the activation of cyclic tertiary *N*-arylamines to generate 1,3-bis radical donors that react with ester activated allylic radical traps acting as 1,3-bis radical acceptors. This formal [3 + 3] annulation reaction relies on the regioselective radical formation at the α and α' positions of the amine, on a rapid 6-*endo*-cyclization that outcompetes intermolecular processes, and on the fact that the final azabicycles are not undergoing further oxidation.

Results and discussion

Proof of concept and optimization. To prove the validity of the annulation approach, *N*-phenylpyrrolidine **1a** was reacted in 1,2-dichloroethane (DCE) with a series of allyl radical traps possessing different leaving groups *Y* in the presence of different

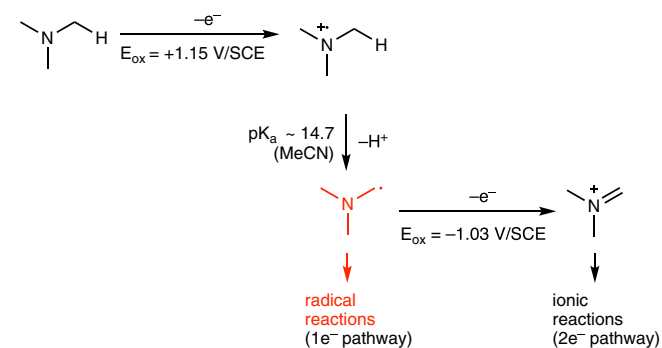


Fig. 3 Oxidation of trimethylamine. One- vs. two-electron pathways. Desired radical process indicated in red.

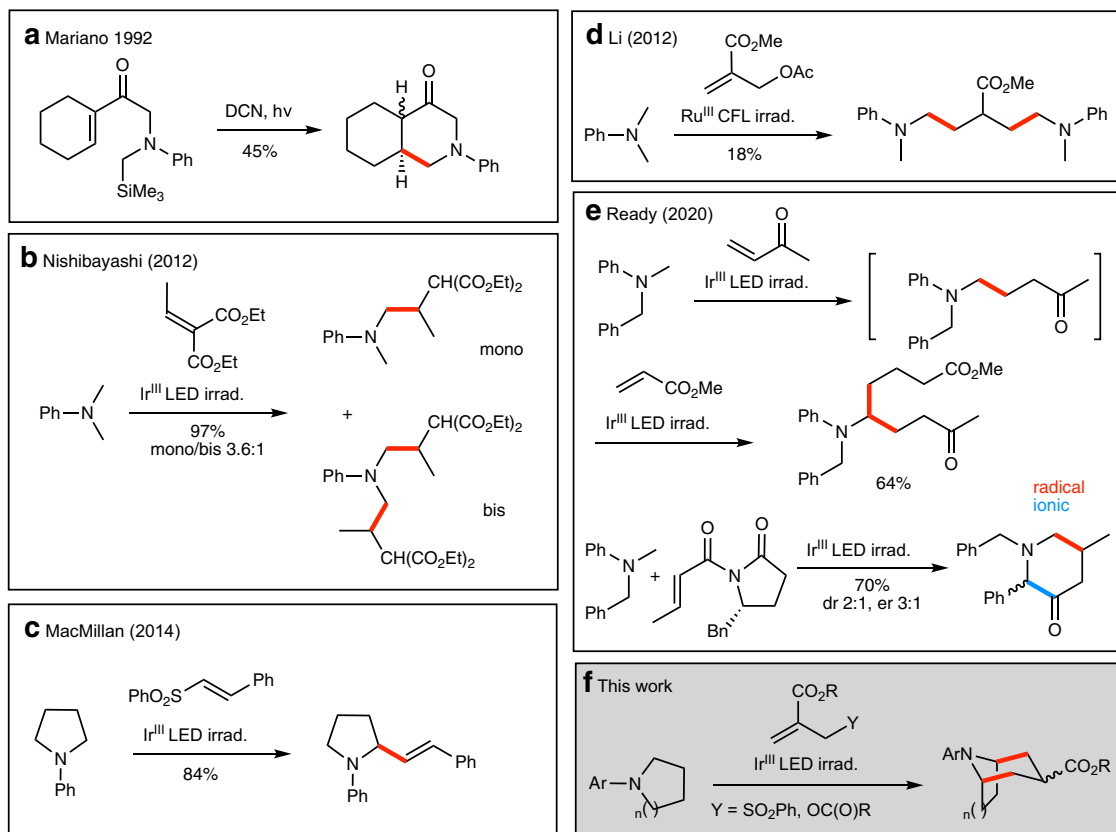
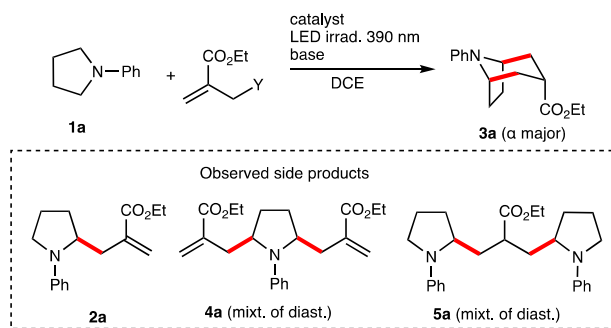


Fig. 4 Photoredox catalyzed α -functionalization of tertiary amines. Selected leading contributions in the field (a–e) and proposed annulation strategy (f). New C–C bonds are indicated in red (radical process) and in blue (ionic process).

Table 1 Optimization of the reaction conditions.

Entry	Cat (mol%)	Base (equiv)	Y (equiv)	Time	[1a]	Yield ^a	Side product
1	Ir-A (2)	CsOAc (3.0)	SO ₂ Ph (1.2)	16 h	0.1 M	45% ^b	4a, 5a
2	Ir-A (2)	CsOAc (1.2)	SO ₂ Ph (1.2)	16 h	0.1 M	59% ^b	4a, 5a
3	Ir-A (2)	CsOAc (1.2)	SO ₂ Ph (1.4)	16 h	0.1 M	65% ^b 43% ^{c,d}	4a, 5a
4	Ir-B (2)	CsOAc (1.2)	SO ₂ Ph (1.4)	16 h	0.1 M	47% ^b	4a, 5a
5	Ir-B (2)	NaOAc (1.2)	SO ₂ Ph (1.4)	16 h	0.1 M	-	2a (26%) ^b
6	Ir-B (2)	Cs ₂ CO ₃ (1.2)	SO ₂ Ph (1.4)	16 h	0.1 M	-	2a (31%) ^b
7	Ir-C (2)	CsOAc (1.2)	SO ₂ Ph (1.4)	16 h	0.1 M	50% ^b	4a, 5a
8	Ru-A (2)	CsOAc (1.2)	SO ₂ Ph (1.4)	16 h	0.1 M	30% ^b	2a (30%) ^b
9	4CzIPN (2)	CsOAc (1.2)	SO ₂ Ph (1.4)	16 h	0.1 M	21% ^b	2a (31%) ^b
10	Eosin Y ^e (2)	CsOAc (1.2)	SO ₂ Ph (1.4)	16 h	0.1 M	-	2a (51%) ^b
11	Ir-A (2)	CsOAc (1.2)	OAc (1.4)	8 h	0.1 M	46% ^b	None
12	Ir-A (2)	CsOAc (1.2)	St-Do (1.4)	8 h	0.1 M	51% ^b	None
13	Ir-A (2)	CsOAc (1.2)	Br (1.4)	8 h	0.1 M	-	2a (66%) ^b
14	Ir-A (2)	CsOAc (1.2)	OAc (1.4)	20 min	0.05	52% ^d	4a
15	Ir-A (1)	CsOAc (1.2)	OAc (1.4)	20 min	0.05	58% ^{c,d}	4a
16	Ir-A (1)	CsOAc (1.2)	OAc (1.1)	20 min	0.05	57% ^d	-
17	Ir-A (1)	CsOAc (1.2)	OPiv (1.1)	20 min	0.05	45% ^d	-
18	Ir-A (1)	CsOAc (1.2)	OTFA (1.1)	2 h	0.05	27% ^d	-

New C-C bonds are indicated in red.

^aReactions run on 0.2 mmol scale.

^bYield for the major diastereomer determined on the crude product by ¹H-NMR analysis using ethylene carbonate as a standard. Levels of diastereoselectivity ranging from 5:1 to 7:1.

^cAverage of three runs.

^dIsolated yield.

^eIrradiation at 325 nm in DMF as a solvent.

catalysts and base additives. The results are collected in Table 1 (more entries are available in the supporting information). Three side products were identified during this optimization phase: the mono-allylated product **2a** (an intermediate in the reaction leading to **3a**), the α,α'-bis-allylated product **4a** and the bis-addition product **5a**. Since all these side products are difficult to separate from the desired tropane **3a**, conditions were sought to minimize their formation. We started the optimization by using ethyl 2-((phenylsulfonyl)methyl)acrylate (Y = SO₂Ph, 1.2 equivalents) as a trap under conditions similar to the one reported in the literature for reactions with vinyl sulfones (see Scheme 3 C)³⁵, i.e., by using [Ir(dF(CF₃)ppy)₂(dtbbpy)]PF₆ (Ir-A) as a catalyst, CsOAc (3 equivalents) as a base and irradiating with 390 nm LEDs in 1,2-DCE (Table 1, entry 1). Gratifyingly, the reaction afforded the desired tropane **3a** in 45% yield (all yields determined by ¹H-NMR analysis using an internal standard). Decreasing the base loading to 1.2 equivalents (Table 1, entry 2) and slightly increasing the amount of the allylsulfone to 1.4 equivalents proved to be beneficial and the product was formed in 65% yield (Table 1, entry 3). However, under these conditions, the product was contaminated with **4a** and **5a** leading to difficult isolation (isolated yield of 43%). The readily available catalyst [Ir(dtbbpy)(ppy)₂]PF₆ (Ir-B) proved to be a suitable catalyst for the reaction, yielding the cyclized product in 47% yield (Table 1, entry 4). A screening of bases revealed that CsOAc was the optimal base. The use of NaOAc and Cs₂CO₃ gave low yields of

mono-allylated pyrrolidine **2a** (Table 1 Entries 5 and 6). The use of [Ir(dFppy)₂(dtbbpy)]PF₆ (Ir-C) afforded the cyclic product **3a** in 50% yield (Table 1, entry 7). Other catalysts presenting suitable redox properties were also tested (for redox properties of the tested catalysts, see supporting information). Ru(bpy)₃(PF₆)₂ (Ru-A) and 2,4,5,6-tetrakis(9H-carbazol-9-yl) isophthalonitrile (4CzIPN) afforded the bicycle **3a**, together with significant amounts of mono-allylated intermediate **2a** (Table 1, entries 8–9). Eosin Y provide only the mono-allylated product **2a** (51% yield, Table 1, entry 10). The influence of the radical trap was investigated next. Pleasingly, ethyl 2-(acetoxymethyl)acrylate³⁶ (Y = OAc) gave the desired product in shorter reaction time (Table 1, entry 11) and similar yield than that with the sulfone trap (Table 1, entry 3). The corresponding sulfide trap (Y = S-*tert*-dodecyl) provided also the desired cyclized product in satisfactory yield (Table 1, Entry 12). However, product isolation was more difficult and the release of one equivalent of a smelly thiol makes the reaction less attractive. Finally, the allyl bromide (Y = Br) was tested and only intermediate **2a** was obtained, with no further conversion to the tropane skeleton **3a** (Table 1, Entry 13). Other catalysts (organic photocatalysts), bases (Na₂CO₃, K₂CO₃) and solvents (DMF, DME, EtOAc, DCM or MeCN) were tested but were all detrimental to the formation of **3a** (see supporting information). Due to shorter reaction time and cleaner product formation, the reaction was further optimized using the allyl acetate trap and catalyst Ir-A. The formation of the bis-allylated product **4a** and the bis-

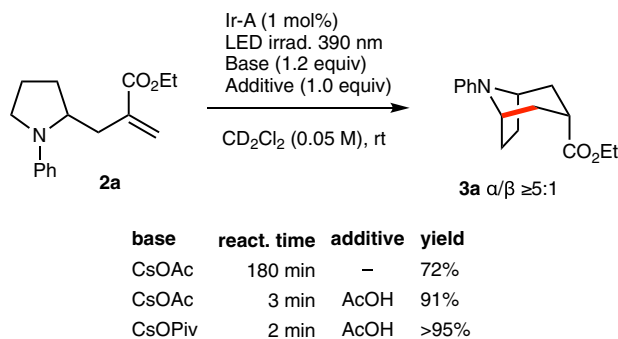


Fig. 5 Cyclization of the mono-allylated pyrrolidine 2a. Influence of acid additives on the cyclization step. New C–C bonds are indicated in red.

addition product **5a** could be minimized by working under higher dilution (0.05 M) and a much shorter reaction time of 20 min (Table 1, entry 14). Reducing the catalyst loading to 1 mol% proved beneficial to the reaction (Table 1, entry 15) and using a smaller excess of the allyl acetate radical trap (1.1 equivalents) did not affect the reaction yield (Table 1, entry 16). Finally, the optimized conditions were used with the corresponding pivalate ($Y = \text{OPiv}$) and trifluoroacetate ($Y = \text{OTFA}$) radical traps (Table 1, entries 17 and 18) but the yields were lower, particularly with the trifluoroacetate.

To gain more understanding on the reaction efficiency, cyclization of the pure mono-allylated **2a** product was examined (Fig. 5). The reaction was run in deuterated dichloromethane under identical conditions (catalyst and base) than the annulation process and was monitored by $^1\text{H-NMR}$. Full conversion of **2a** was achieved after 3 h of irradiation and the bicyclic product **3a** resulting from a 6-*endo* cyclization was obtained in 72% yield. The long reaction time necessary to reach full conversion was puzzling since the overall one-pot annulation process was complete within less than 20 minutes. Since acetic acid (one equivalent) is generated during the allylation step leading to **2a**, the reaction was repeated in the presence of one equivalent of acetic acid. Remarkably, the cyclization was finished in 3 min and an improved yield of 91% was obtained. Running the reaction with CsOPiv (1.2 equiv) and acetic acid (1.0 equiv) afforded the cyclized product in nearly quantitative yield within 2 min. This is in accordance with findings reported by Yoon et al. where their photocatalytic addition of α -aminoalkyl radicals on Michael acceptors was improved by the addition of a Brønsted acids such as TFA³⁸.

Adding acetic acid (1 equiv) to the one-pot annulation reaction either at the beginning or during the reaction did not improve the yield indicating that the in situ generated acetic acid was sufficient for the whole process to occur. Running the reaction with CsOPiv (1.2 equivalents) as a base gave results very similar to CsOAc. Overall, these findings show that the optimized conditions for the annulation reaction (Table 1, entry 16) do not need to be modified.

Reaction scope. The scope of the reaction was examined using the optimized reaction conditions. At first, different *N*-arylpiperidines **1a–e** were examined (Fig. 6). The reaction works well with *p*-substituted *N*-arylpiperidines leading to **3a–3d** in 42–57% yield and good levels of diastereoselectivity in favor of the α isomer ($\alpha/\beta \geq 5:1$). The relative configuration of the **3a** was determined by single crystal X-ray diffraction crystallography. Interestingly, the electron rich *N*-*p*-methoxyphenylpyrrolidine required longer reaction time despite the fact that this compound is more easily oxidizable, indicating that the critical step of the reaction is probably the deprotonation of the radical cations

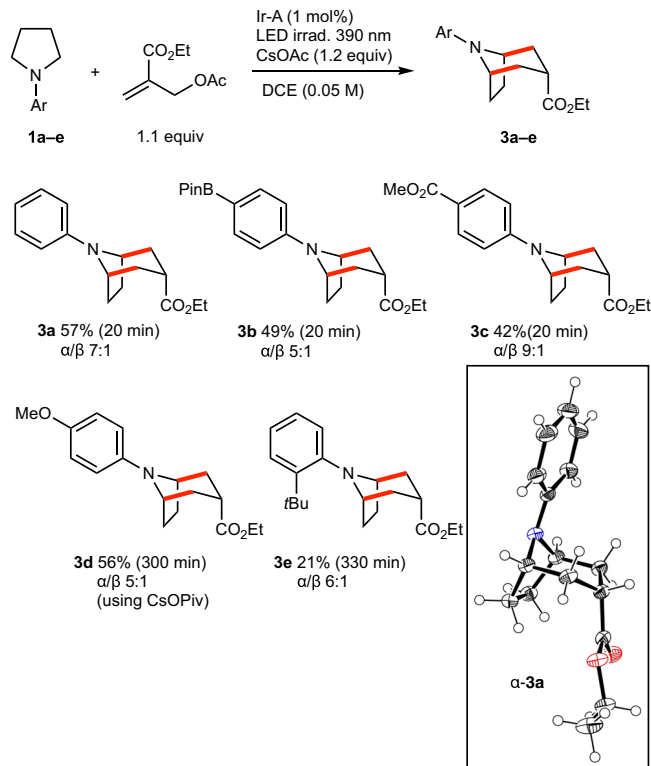


Fig. 6 Tropane skeletons via radical annulation. Scope of the *N*-aryl moiety. New C–C bonds are indicated in red. X-ray crystal structure of **3a** (ellipsoids drawn at 50% probability).

leading to the α -aminoalkyl radicals as discussed by Mariano in his early work (see a discussion of the mechanism, *vide infra*)^{39,40}. In this particular case, the use of the slightly more basic CsOPiv instead of CsOAc provided **3d** in a good 56% yield. The presence of *ortho*-substituent proved to be more problematic as shown by the long reaction time and low yield (20%) observed for the formation of **3e**.

Next, the use of a 2-substituted pyrrolidine was examined. For this purpose, the 2-methyl substituted *N*-phenylpyrrolidine **1f** was prepared and submitted to our standard reaction conditions (Fig. 7). It afforded the desired bicyclic **3f** containing a quaternary carbon at the bridgehead position in 40% yield. This result was surpassing our expectation since a difficult regioselectivity control was expected for the second step of the process, i.e., the conversion of **2f** to **3f** via 6-*endo*-trig cyclization. A study of this cyclization showed that **3f** could be obtained from **2f** in 66% isolated yield indicating that the desired α -amino- α -methyl radical **R2f** was preferentially formed over **R2f'**. This cyclization yield compared well with the non-methylated substrate **2a** that afforded **3a** in 77% isolated yield.

Encouraged by these results, we then turned our attention to the preparation of the homotropane 9-azabicyclo[3.3.1]nonane skeleton as well as higher [4.3.1]-analogues (Fig. 8). Piperidine derivatives proved in general to react slightly better than pyrrolidine derivatives. *N*-Phenylpiperidine **6a** gave the cyclized product **8a** in 67% yield (56% on 3 mmol scale) with an excellent level of diastereoselectivity ($\alpha/\beta > 20:1$). The *N*-toluyl derivatives **8b–8d** were obtained in similar yields and levels of diastereoselectivity. The electron rich *N*-*p*-anisyl derivatives in the presence of CsOPiv as a base required longer reaction time and afforded **8e** in lower yield (32%). Aromatic rings substituted by electron withdrawing groups afforded the homotropanes **8f–8j** in good yields and shorter reaction times in most cases. The *p*-ester

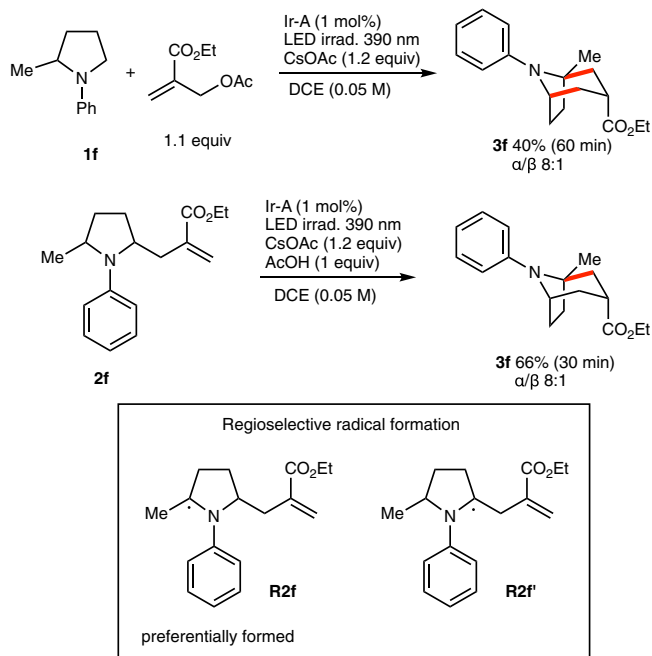


Fig. 7 Annulation reaction of *N*-phenyl-2-methylpyrrolidine. New C–C are indicated in red. The reaction involves the regioselective activation of 2,5-disubstituted pyrrolidine to form preferentially **R2f** over **R2f'**.

substituted homotropane **8g** was prepared 63% yield on 1 mmol scale and the *p*-pinacolboronyl derivative **8j** in 58% yield on 3 mmol scale. Gratifyingly, in all the scale-up experiments for **8a**, **8g** and **8j**, the catalyst loading could be decreased to 0.5 mol%. The relative α -configuration of **8g** was confirmed by single crystal X-ray diffraction crystallography. Annulations starting from *N*-phenylmorpholine, *N*-phenylpiperazine and *N*-phenylthiomorpholine derivatives **6k–m** provided the bicyclic amines **8k–m** in good yields. Remarkably, no products arising from the ring-opening of the piperazine⁴¹ and thiomorpholine^{42,43} were observed. Finally, the reactivity of azepane derivatives were investigated. The *N*-phenyl derivative **6n** gave the bicyclic amine **8n** in a modest 25% yield after 14 h. When the reaction was stopped after 10 min, the allylated product **7n** was obtained in 65% yield together with some cyclized product indicating that the 6-*endo* cyclization was probably the yield limiting step. This was confirmed by an independent cyclization attempt starting from **7n** that afforded **8n** in 24% yield after two hours, along with 9% unreacted **7n** and some unidentified side products. The *N*-(*p*-methoxycarbonylphenyl) derivative **6o** was also examined. After 9 h of reaction, only the allylated product **7o** was formed in a low 25% yield and incomplete conversion.

2-Alkyl-3-ethoxycarbonyl substituted tropanes and homotropanes are expected to be accessible by using easily available acetylated Baylis–Hillman adducts. In order to test this hypothesis, ethyl 2-(1-acetoxyethyl)acrylate was prepared from the ethyl acrylate and acetaldehyde and reacted with *N*-(*p*-

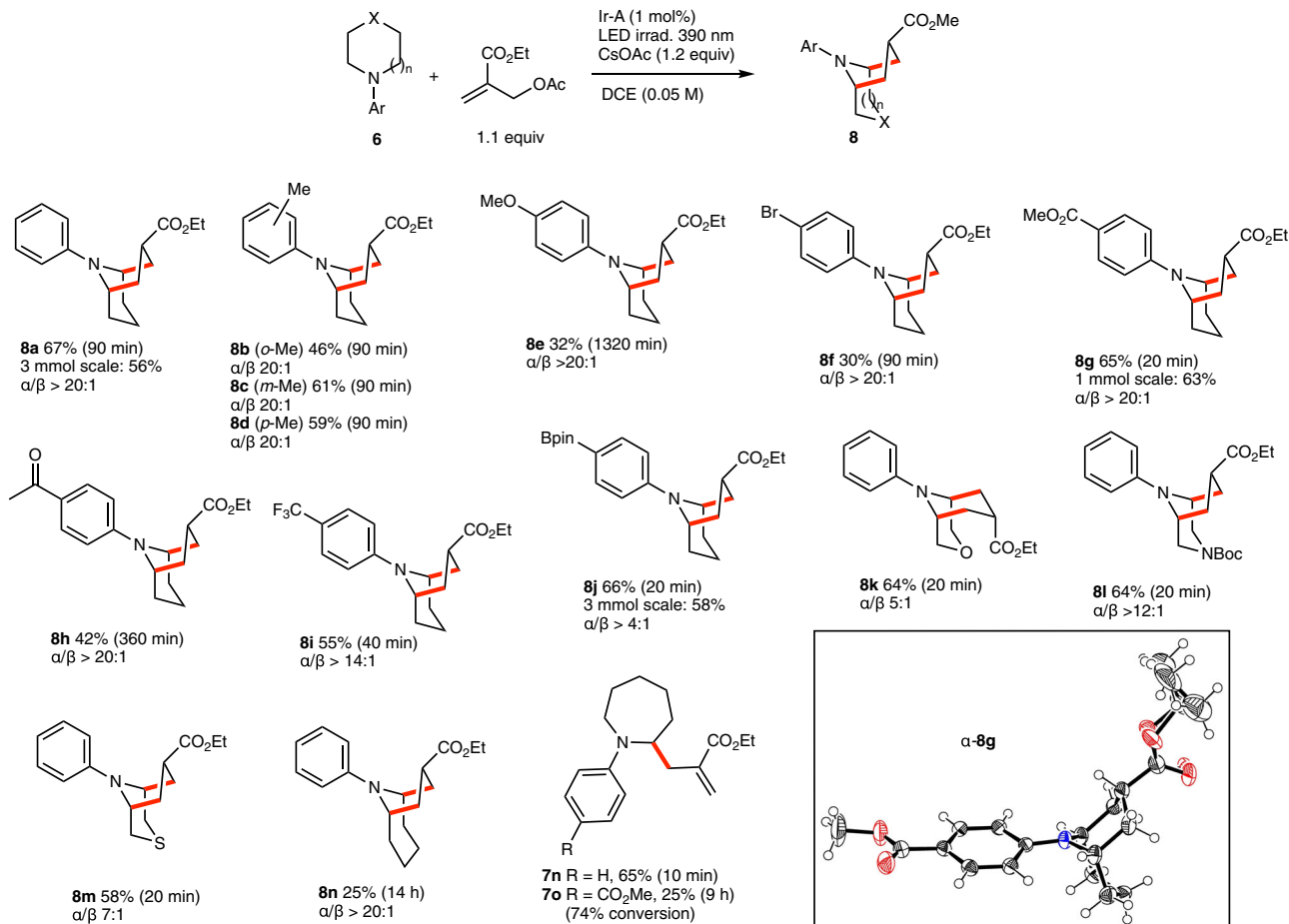


Fig. 8 Homotropane [3.3.1] and extended tropane [4.3.1] skeletons. New C–C bonds are indicated in red. Products are drawn in their major conformations attributed from ¹H-NMR spectra analysis. X-ray crystal structures of α -**8g**, ellipsoids drawn at 50% probability (oxygen and nitrogen atom are represented in red and blue, respectively).

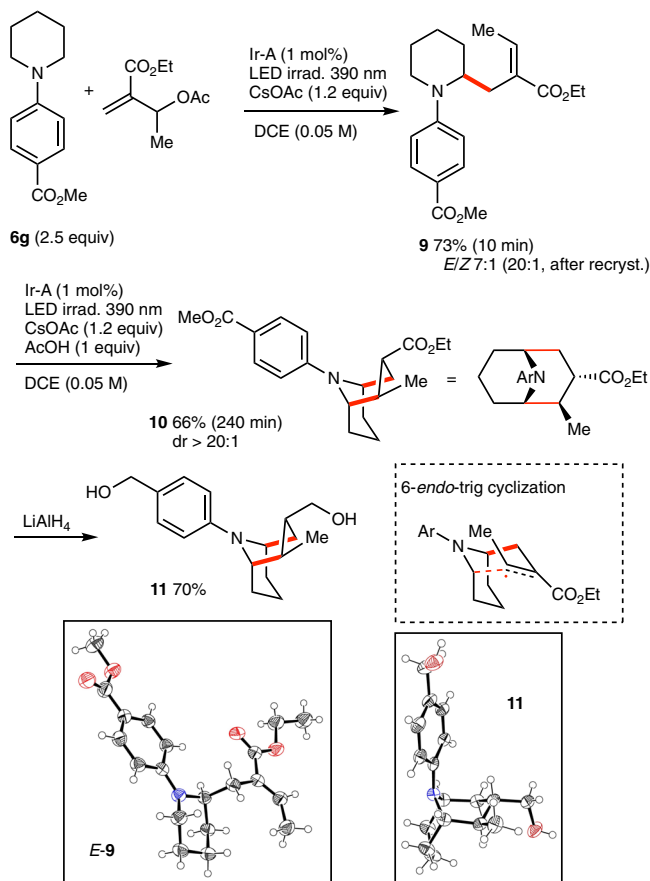


Fig. 9 2,3-Disubstituted [4.4.1]-homotropane. Diastereoselective preparation of a 2,3-disubstituted [4.4.1]-homotropane. New C-C are indicated in red. X-Ray crystal structure of *E*-**9** and **1**, ellipsoids drawn at 50% probability.

methoxycarbonylphenyl)piperidine **6g** (Fig. 9). When 1.1 equivalent of the trap was employed under our standard reaction conditions, prolonged irradiation afforded a mixture of the desired tropane skeleton **10** together with mono-allylated piperidine **9** and the bis-allylated product. Using a 2.5 fold excess of the amine allowed for the formation of the bis-allylated product to be suppressed and, after 10 min of irradiation, the intermediate **9** was obtained in 73% yield and with a good *E*-stereoselectivity (*E/Z* 7:1). Recrystallization of **9** afforded a virtually diastereomerically pure product (*E/Z* > 20:1). Gratifyingly, under our optimized cyclization conditions the major *E*-**9** afforded **10** in 66% yield and as a single diastereomer (*dr* > 20:1). However, despite the good results obtained for both steps separately, the one-pot process provided a mixture of **9** and **10**. This mixture can be treated under the cyclization conditions to ultimately give the cyclized product **10** in 71% yield contaminated with a by-product, presumably a diastereomer. The diester **10** was converted to corresponding diol **11** whose relative configuration could be determined by single crystal X-ray diffraction crystallography (Fig. 9). The formation of the major diastereomers results presumably from a chair-like transition state as depicted in Fig. 9.

Since most of the bicyclic alkaloids are either secondary amines (nortropans, homotropans) or *N*-methylated tertiary amines (tropans), it is important to achieve the deprotection of the *N*-aryl moiety. Methoxyphenyl substituents can be removed under oxidative conditions using chemical oxidants such as cerium ammonium nitrate (CAN) or electrochemical methods⁴⁴.

The cleavage of the *N*-*p*-MeOPh group of **3c** and **8e** was investigated first and proved to be problematic when an aqueous CAN solution was used⁴⁵ as the quinone liberated during the process reacted with the liberated secondary amines. Gratifyingly, the deprotections were successfully achieved using CAN in $\text{CH}_3\text{CN}/\text{water}$ followed by subsequent treatment of the reaction mixture with sodium borohydride to reduce the quinone, then with benzyl chloroformate to prepare their *N*-Cbz-protected form⁴⁶. Under these conditions, the desired Cbz-protected nortropane **12** and homotropane **13** were obtained in 90% and 80% yields, respectively, without erosion of the diastereomeric ratio (Fig. 10a). The Cbz-protecting group was introduced to facilitate product purification but also for both its facile deprotection and conversion to the corresponding *N*-methyl derivative⁴⁷. Since annulation reactions with the *N*-*p*-MeOPh substituted cyclic amines were slow and moderately efficient, we also investigated the deprotection of the *N*-(*p*-pinacolboronyl) phenyl derivative **8j** that was formed in good yield. The dearylation of **8j** to **13** (Fig. 10b) was conveniently performed in 71% yield by sodium perborate treatment, affording after simple extraction the crude phenol, followed by CAN and CbzCl treatment according to the optimized procedure developed for the *para*-methoxy derivatives **3c** and **8e**.

Finally, we hypothesized that the major α -ethoxycarbonyl substituted tropans and homotropans were formed by kinetic protonation of the intermediate enolate from the less hindered *exo*-face (see mechanism, *vide infra*). Epimerization of α -stereoisomers to the more stable β -products was therefore examined. Heating the ester **3a** and **8a** at 40 °C in ethanol in the presence of sodium ethoxide afforded the β isomers in good to excellent levels of diastereoselectivity (Fig. 11). This strategy is expected to be useful for the stereocontrolled synthesis of tropans and homotropane alkaloids.

Mechanism. As mentioned in the introduction, the photocatalytic generation of α -aminoalkyl radicals from cyclic anilines and their subsequent intermolecular addition to Michael acceptors are well-established processes. However, the selectivity of the reaction sequence responsible for the annulation process is quite unique and deserves to be discussed (Fig. 12). Upon blue light irradiation the catalyst Ir-A reaches its excited state $\text{Ir(III)}^*(E_{\text{ox}}^* \text{ Ir(III)}^*/\text{Ir(II)}) = +1.21 \text{ V SCE in MeCN}$ ⁴⁸ and is able to oxidize *N*-phenylpyrrolidine **1a** to its aminium radical cation **RC1a** ($E_{\text{red}} = +0.62 \text{ V/SCE in MeCN}$), which generates the α -aminoalkyl radical **R1a** upon deprotonation. This nucleophilic radical adds to the electron-poor double bond of the allylic trap, leading to an intermediate α -ester radical **RE2a**. The reduction potential of the tertiary radical **RE2a** is estimated to be $E_{\text{red}} > -0.29 \text{ V SCE}$ (see supporting information for details). Such a radical is expected to be readily reduced by the Ir(II) species ($E_{\text{red}} \text{ Ir(III/II)} = -1.37 \text{ V/SCE}$)⁴⁸, thus closing the first catalytic cycle and providing a transient enolate intermediate that produces the mono-allylated pyrrolidine **2a** upon β -fragmentation. The intermediate **2a** is now able to enter the second catalytic cycle. After oxidation of **2a** and subsequent deprotonation, the α -aminoalkyl radical **R2a** is formed selectively. The latter undergoes a 6-*endo*-trig cyclization, leading to the bicyclic α -ester radical **RE3a** whose calculated reduction potential ($E_{\text{red}} = -0.77 \text{ V SCE}$, see supporting information for details) is in good agreement with the experimental value of $E_{\text{red}} = -0.66 \text{ V SCE}$ reported for the secondary α -ester radical $\text{CH}_3\text{CH}(\bullet)\text{CO}_2\text{Me}$ ⁴⁹. This allows for its facile reduction by the Ir(II) species, thus closing the second catalytic cycle. *exo*-Selective protonation of the transient enolate ultimately delivers the desired bicyclic product **3a**.

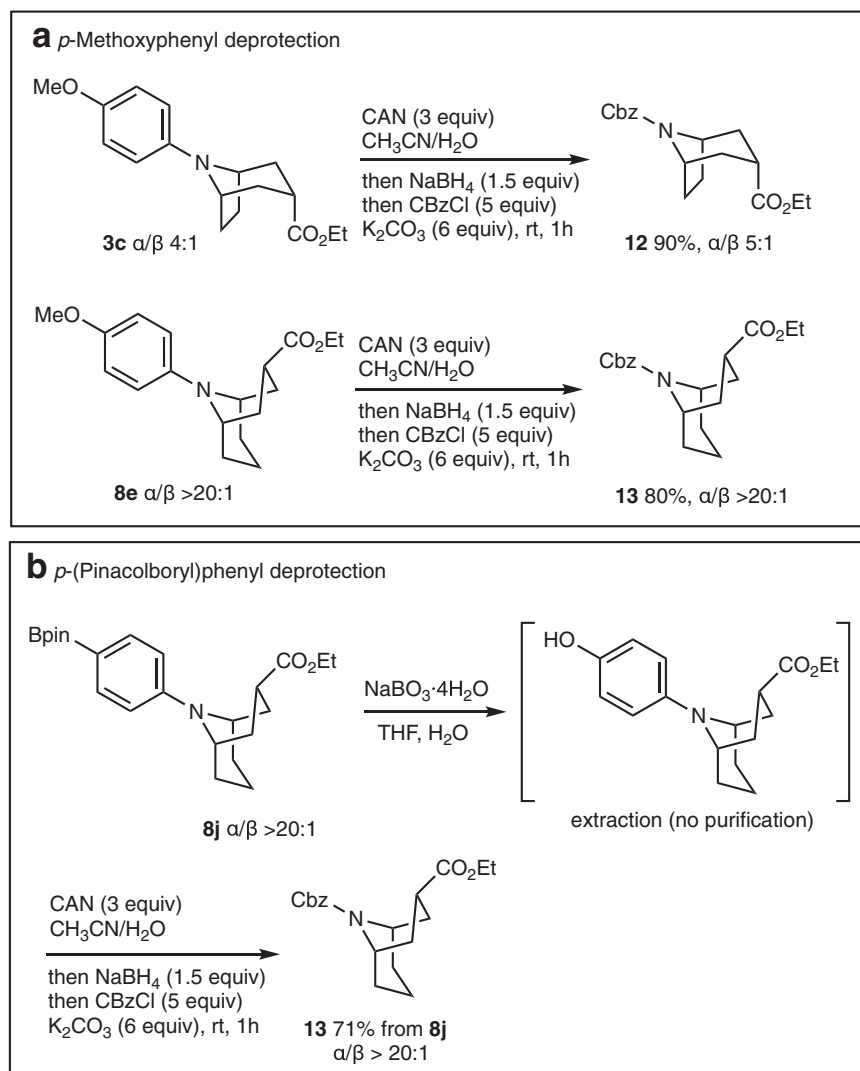


Fig. 10 N-Dearylation. Dearylation of (a) the *N*-MeOPh derivative **3c** and **8e**, and (b) the *N*-*p*-pinBPh derivative **8j**.

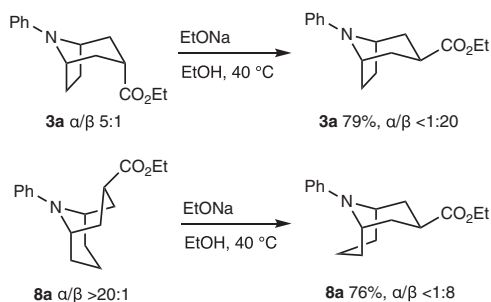


Fig. 11 Epimerization. Base promoted thermodynamic epimerization of tropane and homotropane derivatives.

The success of this approach relies on three key features. Firstly, the radical cation **RC2a** needs to be regioselectively deprotonated to form the radical **R2a**. No product resulting from **R2a'** has been identified but we cannot exclude that such products are formed in small amount (Fig. 12a). The calculated pK_a values for the C(2)-H and C(3)-H bond (see scheme 11 A) are very close and cannot be used to rationalize this result. Nevertheless, this type of selectivity for the less substituted position is well-established and can be rationalized by both steric

and stereoelectronic effects^{25,50–54}. Secondly, in principle all three amines **1a**, **2a** and **3a** present in solution can be easily oxidized by the Ir(III)* catalyst excited state. However, only **RC1a** and **RC2a** (calculated pK_a 51.4 and 52.7 in DCE) are undergoing deprotonation to generate α -aminoalkyl radicals. The deprotonation of the bicyclic radical **RC3a** (pK_a 58.4) is much less favorable and no product resulting from the bicyclic radical **R3a** has been observed (Fig. 12b). A separate attempt to achieve allylation of pure **3a** under our standard reaction conditions led only to partial decomposition of the starting material without formation of an allylated product. Since the oxidation potentials of all three amines **1a**, **2a** and **3a** are close and well below the oxidation potential of the excited Ir(III)* catalyst, we believe that the efficacy of the whole process is due to the fact that oxidation of **3a**, which is becoming increasingly important as the reaction proceeds, is not leading to its decomposition as long as **1a** and **2a** are present in solution due to rapid electron transfers between the different amines in solution (Fig. 12c). Such rapid electron transfers involving radical cations are well-documented in the literature^{55–57} and have led to the use of triarylaminium radical cation as organic mediator in electro-organic synthesis^{58–61}.

The proposed mechanism suggests that the efficiency of the annulation process is dictated by the formation of a final product that cannot deliver efficiently an α -aminoalkyl radical due to an unfavorable (or less favorable) deprotonation step. This may

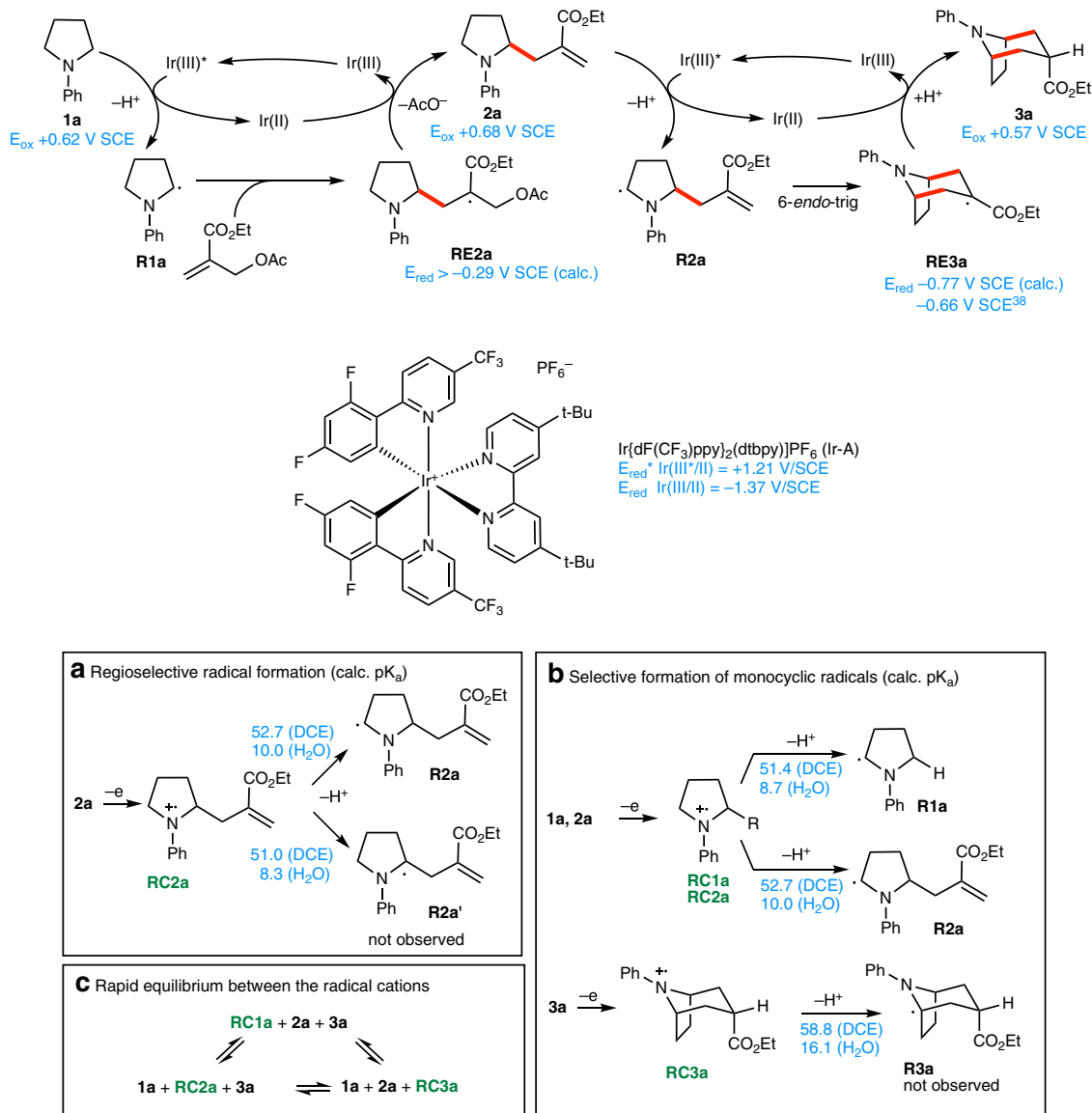


Fig. 12 Mechanism. Possible mechanism for the [3 + 3] radical annulation and analysis of (a) the regioselectivity of radical formation, (b) the selective formation of bicyclic radicals, and (c) the equilibrium between the different radical cations formed during the reaction. New C–C bonds are indicated in red. Redox potentials and pK_a s are indicated in blue. Radical cations are labeled in green.

explain the difficulties and low yields observed in the annulation of azepanes leading to [4.3.1] bicycles (see formation of **8n** in Fig. 8), for which the larger bicyclic systems are expected to favor deprotonation due to an increase of conformational flexibility leading to product and catalyst degradation. This assumption is supported by calculations, the oxidation potential of **8n** ($E_{ox} + 0.66 V/SCE$) lying within the range of our catalyst and the pK_a of the corresponding radical cation **RC8n** (pK_a 49.5 (DCE), 6.8 (H₂O)) being far below the ones of the less flexible **RC3a** (pK_a 58.8 (DCE), 16.1 (H₂O)) and **RC8a** (pK_a 57.1 (DCE), 14.4 (H₂O)) and similar to the one of the monocyclic amines.

Counter-intuitively, the reactions with electron-enriched aniline systems such as *N*-(*para*-methoxyphenyl)pyrrolidine **1d** (to form **3d**, see Fig. 6) and *N*-(*para*-methoxyphenyl)piperidine **6e** (to form **8e**, Fig. 8) were more difficult than those with electron-poorer systems. They required much longer reaction times and, in the case of **1d**, the use of a slightly stronger base. This indicates that the critical step of the process is probably not the amine oxidation but rather the deprotonation of the radical cation. Calculations showed that the

more stable *para*-methoxyphenyl substituted radical cation **RC1d** is also much less acidic ($pK_a = +57.1$ (DCE)/+14.4 (H₂O)) than **RC1a** ($pK_a = +51.4$ (DCE)/+8.7 (H₂O)). The electrochemical investigation of **1d** by cyclic voltammetry provided a quasi-reversible oxidation wave in the absence of added base (Fig. 13a) whilst the simple *N*-phenylpyrrolidine **1a** produced irreversible oxidation event (see supporting information)^{62,63}. The addition of cesium pivalate drastically changed the cyclic voltammogram of **1d** and two oxidation waves were observed (Fig. 13b). A first irreversible oxidation wave appeared at a slightly lower oxidation potential than the oxidation event of the amine alone. This shift of potential relative to the cyclic voltammogram in the absence of base is attributed to an oxidation event of the amine interacting with cesium pivalate, possibly a proton-coupled electron transfer process^{64,65}. The second wave, whose potential corresponds to the oxidation event observed in the absence of base, becomes less reversible in presence of cesium pivalate. The voltammogram of the tropane **3d** (Fig. 13c) indicates as anticipated a reversible oxidation process. Interestingly, it is almost not affected by the presence of cesium pivalate indicating that the

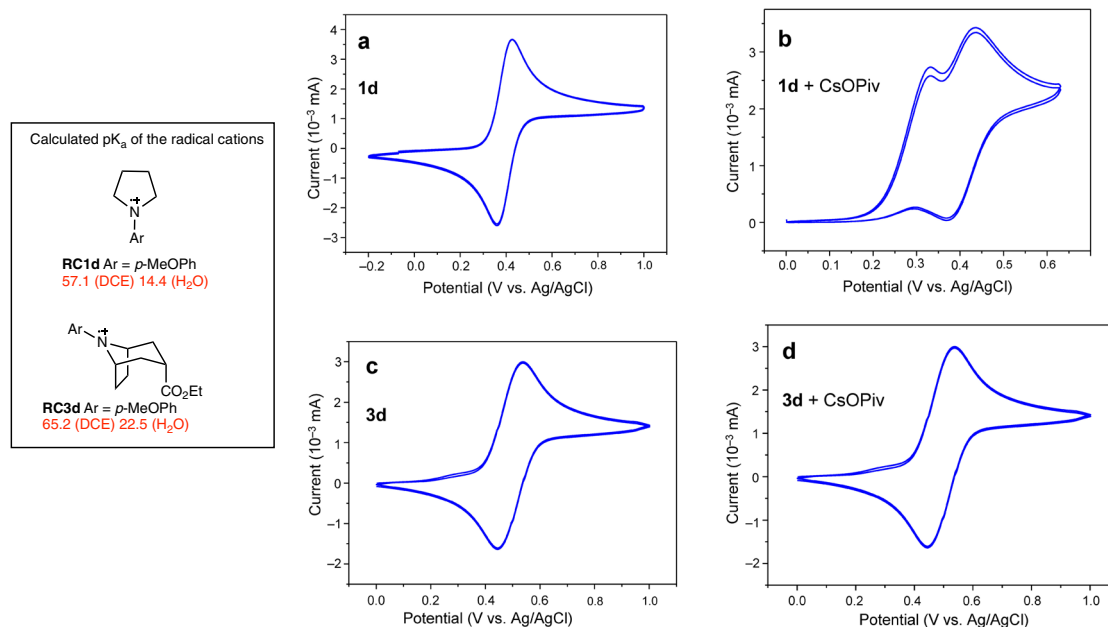


Fig. 13 Electrochemical study. Cyclic voltammograms of *N*-*p*-methoxyphenylamines **1d** and **3d** (1 mM) in the absence (**a** and **c**) and in the presence of cesium pivalate (1.2 mM) (**b** and **d**). Voltammograms were recorded at 100 mV/s in acetonitrile containing [Bu₄N][PF₆] (0.1 M) as a supporting electrolyte. pK_as are indicated in red. Voltammogram traces are depicted in blue.

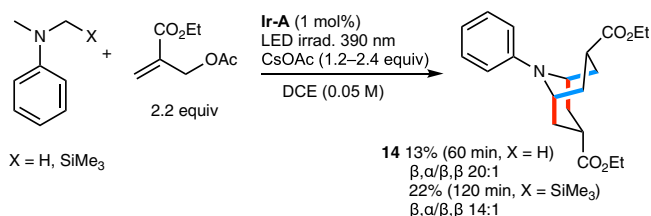


Fig. 14 Double annulation process. Synthesis of a homotropane skeleton via a double [3 + 3] annulation reaction. C–C Bonds formed during the first annulation process are indicated in red, C–C Bonds formed during the second annulation process are indicated in blue.

bicyclic cation radical of **3d** is not deprotonated by the base during the measurement (Fig. 13d). This observation supports the proposed mechanism and the fact that the photoredox annulation process stops at the bicyclic stage.

The hypothesis that the reactions stop at the bicyclic stage due to inefficient deprotonation of the bicyclic radical cation offers the opportunity to run a more complex reaction process involving a bis-annulation process starting from a tertiary acyclic aniline derivative and ending with an oxidation-resistant bicyclic system. This assumption was tested with *N,N*-dimethyl aniline. In the presence of 2.2 equivalents of the allylic acetate radical trap added in two portions (at the beginning of the reaction and after 15 min), the product of bis-annulation product **14** was isolated in 13% yield with good stereocontrol. By starting from *N*-methyl-*N*-trimethylsilyl-methylaniline, the yield for the formation of **14** could be improved to 22%. In this process, the product of the first annulation (Fig. 14, blue bond formation) leads to a piperidine derivative that can further react via a second annulation process (Fig. 14, red bond formation) to produce **14**. All attempts to stop at the piperidine stage gave complex inseparable mixture of products.

Conclusion

In summary, we have developed a new annulation strategy for the synthesis of bicyclic alkaloid skeletons. The reactions take place

under mild conditions and afford *N*-arylated tropane and homotropane frameworks in good yields and good to excellent levels of diastereoselectivity starting from simple and readily available starting materials using visible-light photoredox catalysis. This annulation process takes advantage of the unique reactivity of ethyl 2-(acetoxymethyl)acrylate as a 1,3-bis radical acceptor and of cyclic *N,N*-dialkylanilines as radical 1,3-bis radical donor. This method complements nicely the classical Robinson synthesis by allowing to prepare directly the biologically relevant *N*-arylated skeletons and by introducing an ester group at position 3 suitable for further derivatization toward application in medicinal chemistry. Preliminary results with differently 2-substituted allyl acetates indicate that the ester group can be substituted by other electron withdrawing groups such as a nitrile, a sulfone and a boronic ester. Details will be reported in due time together with the synthesis of optically pure biologically relevant compounds.

Methods

General procedure. In an oven-dried 10 mL vial were successively added ethyl 2-(acetoxymethyl)prop-2-enoate (0.22 mmol, 1.1 equiv), *N*-arylpiperidine or *N*-arylpiperidine (0.20 mmol, 1 equiv.), [Ir{dF(CF₃)ppy}₂(dtbpy)]PF₆ (2.2 mg, 0.02 mmol, 1 mol%) and cesium acetate (46 mg, 0.24 mmol, 1.2 equiv.). The vial was closed with a rubber septum and evacuated/filled with N₂ (3×). Finally, dry and degassed 1,2-DCE (4.00 mL) was added. The resulting yellow mixture was placed 5 cm away from a 390 nm blue LED and stirred until completion of the reaction. Reactions usually turned orange and a fine white precipitate was observed. The reaction mixture was diluted with sat. NaHCO₃ (3 mL) and the aq. phase was extracted with CH₂Cl₂ (3 × 5 mL) and the combined organic phases were dried over Na₂SO₄, filtered, and concentrated under reduced pressure to give crude product as an orange oil. Purification by flash column chromatography on neutral Alox[®] or SiO₂ afforded the bicyclic product. Details including experimental procedures and product characterizations are available in the Supplementary Methods (Supplementary Tables 1–6). Copies of relevant NMR data are available in the Supplementary Note 1.

Calculations. All DFT calculations were performed with the ADF (Amsterdam Density Functional) code developed by E. J. Baerends et al.⁶⁶ using triple-zeta basis sets (no frozen core). Geometry optimizations were performed *in vacuo* relying on the Generalized Gradient Approximation VBP exchange-correlation (XC) potential (VWN and BP by Vosko et al.⁶⁷, corrective terms by Becke⁶⁸ for the exchange and Perdew⁶⁹ for the correlation) with ADF grid precision 6 throughout. Details are available in the Supplementary Methods (Supplementary Figs. 1,2 and Supplementary Tables 7–10).

Cyclic voltammetry. Cyclic Voltammetry experiments were performed in acetonitrile at room temperature in an argon-filled glovebox with 0.1 M of $[Bu_4N][PF_6]$ as a supporting electrolyte. Data were collected using a BioLogic SP-300 potentiostat connected to a three-electrodes system, including a glassy carbon disk ($d = 1$ mm) working electrode, a platinum wire counter electrode, and an Ag/AgCl reference electrode. The voltammograms of each compound were recorded at different scan rates (from 20 mV/s to 20 V/s). The linearity of the oxidation current with the square root of the scan rates was checked for the four compounds in the different experimental cases. Potential calibration was performed at the end of each data collection cycle using the ferrocene/ferrocenium couple as an internal standard ($E^\circ = 0.380$ V/SCE). More details are available in the Supplementary Methods (Supplementary Figs. 3,4 and Supplementary Tables 11).

Data availability

The X-ray crystallographic coordinates for structures reported in this Article have been deposited at the Cambridge Crystallographic Data Centre (CCDC), under deposition number CCDC 2111680 (3a), CCDC 2111681 (α -8g), CCDC 2111682 (E-9), and CCDC 2111684 (11). These data can be obtained free of charge from The Cambridge Crystallographic Data Centre via www.ccdc.cam.ac.uk/data_request/cif. The cif files for 3a, α -8g, 9 and 11 are also available as Supplementary Data 1–4. DFT geometry-optimized coordinates are available in the Supplementary Data 5. Any other relevant data are available from the authors upon reasonable request.

Received: 7 February 2022; Accepted: 25 March 2022;

Published online: 28 April 2022

References

- Kohnen-Johannsen, K. L. & Kayser, O. Tropane alkaloids: chemistry, pharmacology, biosynthesis and production. *Molecules* **24**, 796 (2019).
- Lima, D. J. P., Santana, A. E. G., Birkett, M. A. & Porto, R. S. Recent progress in the synthesis of homotropane alkaloids adaline, euphococcinine and N-methyleuphococcinine. *Beilstein J. Org. Chem.* **17**, 28–41 (2021).
- Goanvic, D. L. & Tius, M. A. Oxaza Adamantyl Cannabinoids. A New Class of Cannabinoid Receptor Probes. *J. Org. Chem.* **71**, 7800–7804 (2006).
- Schlienger, N. et al. Synthesis, Structure–Activity Relationships, and Characterization of Novel Nonsteroidal and Selective Androgen Receptor Modulators. *J. Med. Chem.* **52**, 7186–7191 (2009).
- Sundén, H. et al. Synthesis and Biological Evaluation of Second-Generation Tropanol-Based Androgen Receptor Modulators. *J. Med. Chem.* **58**, 1569–1574 (2015).
- Liu, Y. et al. The Discovery of Orally Bioavailable Tyrosine Threonine Kinase (TTK) Inhibitors: 3-(4-(heterocyclyl)phenyl)-1H-indazole-5-carboxamides as Anticancer Agents. *J. Med. Chem.* **58**, 3366–3392 (2015).
- Robinson, R. LXIII.—A synthesis of tropinone. *J. Chem. Soc. Trans.* **111**, 762–768 (1917).
- Medley, J. W. & Movassaghi, M. Robinson's landmark synthesis of tropinone. *Chem. Commun.* **49**, 10775–10777 (2013).
- Afewerki, S., Wang, J.-X., Liao, W.-W. & Córdova, A. Chapter Three - The Chemical Synthesis and Applications of Tropane Alkaloids. in *The Alkaloids: Chemistry and Biology* (ed. Knölker, H.-J.) 81 151–233 (Academic Press, 2019).
- Willand, N. et al. Efficient, two-step synthesis of N-substituted nortropinone derivatives. *Tetrahedron Lett.* **48**, 5007–5011 (2007).
- Jung, D. et al. Synthesis of N-arylnortropinone derivatives. *J. Korean Chem. Soc.* **41**, 414–419 (1997).
- De Ridder, D. J. A., Goubitz, K., Schenk, H., Krijnen, B. & Verhoeven, J. W. Effect of Through-Bond Interaction on Conformation and Structure in Rod-Shaped Donor–Acceptor Systems. Part 2. *Helv. Chim. Acta* **86**, 812–826 (2003).
- Song, J. H., Bae, S. M., Cho, S. K., Cho, J. H. & Jung, D. I. A Study on N-Substituted Nortropinone Synthesis using Acetone Equivalents. *Asian J. Chem.* **32**, 1145–1150 (2020).
- Hassine, M., Jannet, H. B., Ghermani, N., Alami, M. & Messaoudi, S. Synthesis of N-(Hetero)arylconvolvine Derivatives through a Palladium-Catalyzed Buchwald–Hartwig Cross-Coupling. *Synthesis* **52**, 450–458 (2020).
- Ikeda, M., Kugo, Y., Kondo, Y., Yamazaki, T. & Sato, T. Regioselective synthesis of bridged azabicyclic compounds using radical translocations/cyclisations of methyl 2-alkynyl-1-(o-iodobenzoyl)pyrrolidine-2-carboxylates: a formal total synthesis of (\pm)-epibatidine. *J. Chem. Soc. Perkin 1*, 3339–3344 (1997).
- Huang, J.-P. et al. Tropane alkaloid biosynthesis: a centennial review. *Nat. Prod. Rep.* **38**, 1634–1658 (2021).
- Curran, D. P. Radical Reactions and Retrosynthetic Planning. *Synlett* **1991**, 63–72 (1991).
- Dowd, P. & Zhang, W. Free radical-mediated ring expansion and related annulations. *Chem. Rev.* **93**, 2091–2115 (1993).
- McCarroll, A. J. & Walton, J. C. Organic syntheses through free-radical annulations and related cascade sequences. *J. Chem. Soc. Perkin 1*, 3215–3229 (2001).
- Rheault, T. R. & Sibi, M. P. Radical-Mediated Annulation Reactions. *Synthesis* **2003**, 803–819 (2003).
- Feng, J. & Liu, B. Formal carbo [3+3] annulation and its application in organic synthesis. *Tetrahedron Lett.* **56**, 1474–1485 (2015).
- Chen, J.-R., Yan, D.-M., Wei, Q. & Xiao, W.-J. Photocascade catalysis: a new strategy for cascade reactions. *ChemPhotoChem* **1**, 148–158 (2017).
- Xuan, J., Lu, L.-Q., Chen, J.-R. & Xiao, W.-J. Visible-Light-Driven Photoredox Catalysis in the Construction of Carbocyclic and Heterocyclic Ring Systems. *Eur. J. Org. Chem.* **2013**, 6755–6770 (2013).
- Srivastava, V., Singh, P. K., Tivari, S. & Singh, P. P. Visible light photocatalysis in the synthesis of pharmaceutically relevant heterocyclic scaffolds. *Org. Chem. Front.* (2022) <https://doi.org/10.1039/D1QO01602D>
- Lewis, F. D. Proton-transfer reactions of photogenerated radical ion pairs. *Acc. Chem. Res.* **19**, 401–405 (1986).
- Nakajima, K., Miyake, Y. & Nishibayashi, Y. Synthetic Utilization of α -Aminoalkyl Radicals and Related Species in Visible Light Photoredox Catalysis. *Acc. Chem. Res.* **49**, 1946–1956 (2016).
- Wayner, D. D. M., Dannenberg, J. J. & Griller, D. Oxidation potentials of α -aminoalkyl radicals: bond dissociation energies for related radical cations. *Chem. Phys. Lett.* **131**, 189–191 (1986).
- Condie, A. G., González-Gómez, J. C. & Stephenson, C. R. J. Visible-Light Photoredox Catalysis: Aza-Henry Reactions via C–H Functionalization. *J. Am. Chem. Soc.* **132**, 1464–1465 (2010).
- Freeman, D. B., Furst, L., Condie, A. G. & Stephenson, C. R. J. Functionally Diverse Nucleophilic Trapping of Iminium Intermediates Generated Utilizing Visible Light. *Org. Lett.* **14**, 94–97 (2012).
- Hu, J., Wang, J., Nguyen, T. H. & Zheng, N. The chemistry of amine radical cations produced by visible light photoredox catalysis. *Beilstein J. Org. Chem.* **9**, 1977–2001 (2013).
- Jeon, Y. T., Lee, C. P. & Mariano, P. S. Radical cyclization reactions of alpha-silyl amine alpha,beta-unsaturated ketone and ester systems promoted by single electron transfer photosensitization. *J. Am. Chem. Soc.* **113**, 8847–8863 (1991).
- Pandey, G., Lakshmaiah, G. & Kumaraswamy, G. A new and efficient strategy for non-stabilized azomethine ylide via photoinduced electron transfer (PET) initiated sequential double desilylation. *J. Chem. Soc. Chem. Commun.* 1313–1314 (1992) <https://doi.org/10.1039/C39920001313>
- Kohls, P., Jadhav, D., Pandey, G. & Reiser, O. Visible Light Photoredox Catalysis: Generation and Addition of N-Aryltetrahydroisoquinoline-Derived α -Amino Radicals to Michael Acceptors. *Org. Lett.* **14**, 672–675 (2012).
- Miyake, Y., Nakajima, K. & Nishibayashi, Y. Visible-Light-Mediated Utilization of α -Aminoalkyl Radicals: addition to Electron-Deficient Alkenes Using Photoredox Catalysts. *J. Am. Chem. Soc.* **134**, 3338–3341 (2012).
- Noble, A. & MacMillan, D. W. C. Photoredox α -Vinylation of α -Amino Acids and N-Aryl Amines. *J. Am. Chem. Soc.* **136**, 11602–11605 (2014).
- Dai, X. et al. The Coupling of Tertiary Amines with Acrylate Derivatives via Visible-Light Photoredox Catalysis. *J. Org. Chem.* **79**, 7212–7219 (2014).
- Leng, L., Fu, Y., Liu, P. & Ready, J. M. Regioselective, Photocatalytic α -Functionalization of Amines. *J. Am. Chem. Soc.* **142**, 11972–11977 (2020).
- Ruiz Espelt, L., Wiensch, E. M. & Yoon, T. P. Bronsted Acid Cocatalysts in Photocatalytic Radical Addition of α -Amino C–H Bonds across Michael Acceptors. *J. Org. Chem.* **78**, 4107–4114 (2013).
- Zhang, X. et al. Dynamics of alpha-CH Deprotonation and alpha-Desilylation Reactions of Tertiary Amine Cation Radicals. *J. Am. Chem. Soc.* **116**, 4211–4220 (1994).
- Dombrowski, G. W. et al. Efficient Unimolecular Deprotonation of Aniline Radical Cations. *J. Org. Chem.* **70**, 3791–3800 (2005).
- Cai, S. et al. Visible-Light-Promoted C–C bond cleavage: photocatalytic generation of iminium ions and amino radicals. *Angew. Chem. Int. Ed.* **51**, 8050–8053 (2012).
- Surzur, J.-M., Crozet, M.-P. & Dupuy, C. Synthèse de systèmes thiacyclohexaniques et thiacycloheptaniques par addition radicalaire intramoléculaire du radical thyle. *Tetrahedron Lett.* **12**, 2025–2028 (1971).
- McCourt, R. & Scanlan, E. M. 5-exo versus 6-endo Thiyyl-Radical Cyclizations in Organic Synthesis. *Helv. Chim. Acta* **102**, e1900162 (2019).
- De Lamo Marin, S., Martens, T., Mioskowski, C. & Royer, J. Efficient N-p-Methoxyphenyl Amine Deprotection through Anodic Oxidation. *J. Org. Chem.* **70**, 10592–10595 (2005).
- Xu, G.-Q. et al. Metal-Free α -C(sp³)-H Aroylation of Amines via a Photoredox Catalytic Radical–Radical Cross-Coupling Process. *Org. Lett.* **23**, 2846–2852 (2021).
- Taniyama, D., Hasegawa, M. & Tomioka, K. A facile and efficient asymmetric synthesis of (+)-salsolidine. *Tetrahedron Lett.* **41**, 5533–5536 (2000).
- Sardina, F. J., Howard, M. H., Koskinen, A. M. P. & Rapoport, H. Chiroselective synthesis of nitrogen and side chain modified analogs of (+)-anatoxin. *J. Org. Chem.* **54**, 4654–4660 (1989).

48. Teegardin, K., Day, J. I., Chan, J. & Weaver, J. Advances in Photocatalysis: A Microreview of Visible Light Mediated Ruthenium and Iridium Catalyzed Organic Transformations. *Org. Process Res. Dev.* **20**, 1156–1163 (2016).
49. Bortolamei, N., Isse, A. A. & Gennaro, A. Estimation of standard reduction potentials of alkyl radicals involved in atom transfer radical polymerization. *Electrochim. Acta* **55**, 8312–8318 (2010).
50. Lewis, F. D., Ho, T.-I. & Simpson, J. T. Photochemical addition of tertiary amines to stilbene. Stereoelectronic control of tertiary amine oxidation. *J. Org. Chem.* **46**, 1077–1082 (1981).
51. Barry, J. E., Finkelstein, M., Mayeda, E. A. & Ross, S. D. Products and mechanisms in the anodic oxidation of N,N-dimethylbenzylamine in methanol. *J. Org. Chem.* **39**, 2695–2699 (1974).
52. Ebersson, L. et al. Studies on Electrolytic Substitution Reactions. IX. Anodic Cyanation of Aromatic Ethers and Amines in Emulsions with the Aid of Phase Transfer Agents. *Acta Chem. Scand.* **29b**, 451–456 (1975).
53. Smith, J. R. L. & Masheder, D. Amine oxidation. Part IX. The electrochemical oxidation of some tertiary amines: the effect of structure on reactivity. *J. Chem. Soc. Perkin Trans. 2*, 47–51 (1976).
54. Xie, J., Rudolph, M., Rominger, F. & Hashmi, A. S. K. Photoredox-Controlled Mono- and Di-Multifluoroarylation of C(sp³)-H Bonds with Aryl Fluorides. *Angew. Chem. Int. Ed.* **56**, 7266–7270 (2017).
55. Ledwith, A. Cation radicals in electron transfer reactions. *Acc. Chem. Res.* **5**, 133–139 (1972).
56. Workentin, M. S., Johnston, L. J., Wayner, D. D. M. & Parker, V. D. Reactivity of Aromatic Radical Cations. Rate Constants for Reactions of 9-Phenyl- and 9,10-Diphenylanthracene Radical Cations with Acyclic Amines. *J. Am. Chem. Soc.* **116**, 8279–8287 (1994).
57. Beresford, P., Lambert, M. C. & Ledwith, A. Cation radicals: ring opening of a cyclobutane by electron transfer. *J. Chem. Soc. C Org.* 2508–2510 (1970) <https://doi.org/10.1039/J39700002508>
58. Connelly, N. G. & Geiger, W. E. Chemical Redox Agents for Organometallic Chemistry. *Chem. Rev.* **96**, 877–910 (1996).
59. Steckhan, E. Indirect Electroorganic Syntheses—A Modern Chapter of Organic Electrochemistry [New Synthetic Methods (59)]. *Angew. Chem. Int. Ed. Engl.* **25**, 683–701 (1986).
60. Steckhan, E. Organic syntheses with electrochemically regenerable redox systems. in *Electrochemistry I* (ed. Steckhan, E.) 1–69 (Springer, 1987). https://doi.org/10.1007/3-540-17871-6_11
61. Quiroz-Guzman, M. & Brown, S. N. Tris(4-bromophenyl)aminium hexachloridoantimonate ('Magic Blue'): a strong oxidant with low inner-sphere reorganization. *Acta Crystallogr. C.* **66**, m171–m173 (2010).
62. Seo, E. T. et al. Anodic Oxidation Pathways of Aromatic Amines. Electrochemical and Electron Paramagnetic Resonance Studies. *J. Am. Chem. Soc.* **88**, 3498–3503 (1966).
63. Adams, R. N. Anodic oxidation pathways of aromatic hydrocarbons and amines. *Acc. Chem. Res.* **2**, 175–180 (1969).
64. Nakamura, A., Latif, M. A., Deck, P. A., Castagnoli, N. Jr. & Tanko, J. M. Evidence for a Proton-Coupled Electron Transfer Mechanism in a Biomimetic System for Monoamine Oxidase B. *Catal. Chem. - Eur. J.* **26**, 823–829 (2020).
65. Costentin, C., Robert, M. & Savéant, J.-M. Update 1 of: Electrochemical Approach to the Mechanistic Study of Proton-Coupled Electron Transfer. *Chem. Rev.* **110**, PR1–PR40 (2010).
66. te Velde, G. & Baerends, E. J. Numerical integration for polyatomic systems. *J. Comput. Phys.* **99**, 84–98 (1992).
67. Vosko, S. H., Wilk, L. & Nusair, M. Accurate spin-dependent electron liquid correlation energies for local spin density calculations: a critical analysis. *Can. J. Phys.* **58**, 1200–1211 (1980).
68. Becke, A. D. Density-functional exchange-energy approximation with correct asymptotic behavior. *Phys. Rev. A* **38**, 3098–3100 (1988).
69. Perdew, J. P. Density-functional approximation for the correlation energy of the inhomogeneous electron gas. *Phys. Rev. B* **33**, 8822–8824 (1986).

Acknowledgements

This work was supported by the Swiss National Science Foundation (project 200021L_182078) and the ANR (project ANR-18-CE93-0004) under the Lead Agency and International Co-Investigator Scheme. V.M. and J.-M.M. thank the Labex ARCANE (ANR-11-LABX-0003) and CBH-EUR-GS (ANR-17-EURE-0003) for partial funding.

Author contributions

E.C., F.D., and P.R. designed the synthetic experiments. E.C. executed all the synthetic work and analyzed the data. J.-M.M. performed the calculations in collaboration with V.M., J.A., A.D., and V.M. designed and run the electrochemical studies and analyzed the data. E.C., F.D., and P.R. co-wrote the paper. All the authors discussed the results and commented on the paper.

Competing interests

The authors declare no competing interests.

Additional information

Supplementary information The online version contains supplementary material available at <https://doi.org/10.1038/s42004-022-00671-x>.

Correspondence and requests for materials should be addressed to Vincent Maurel, Jean-Marie Mousca or Philippe Renaud.

Peer review information *Communications Chemistry* thanks the anonymous reviewers for their contribution to the peer review of this work.

Reprints and permission information is available at <http://www.nature.com/reprints>

Publisher's note Springer Nature remains neutral with regard to jurisdictional claims in published maps and institutional affiliations.

 **Open Access** This article is licensed under a Creative Commons Attribution 4.0 International License, which permits use, sharing, adaptation, distribution and reproduction in any medium or format, as long as you give appropriate credit to the original author(s) and the source, provide a link to the Creative Commons license, and indicate if changes were made. The images or other third party material in this article are included in the article's Creative Commons license, unless indicated otherwise in a credit line to the material. If material is not included in the article's Creative Commons license and your intended use is not permitted by statutory regulation or exceeds the permitted use, you will need to obtain permission directly from the copyright holder. To view a copy of this license, visit <http://creativecommons.org/licenses/by/4.0/>.

© The Author(s) 2022